

Acoustic Timescale Detonation Initiation in 2-D and its Implications on the 1-D Description

Jonathan D. Regele
California Institute of Technology
Pasadena, CA USA
David R. Kassoy, Oleg V. Vasilyev
University of Colorado
Boulder, CO USA

1 Introduction

One dimensional numerical simulations of spatially resolved thermal power deposition on the acoustic timescale have demonstrated a mechanism to achieve Deflagration-to-Detonation Transition (DDT) [1, 2]. If the power deposition increases the temperature of a volume of fluid of length l in an amount of time $t_h \sim t_a = l/a$, where t_a is the acoustic timescale and a is the undisturbed speed of sound, the reactants will ignite in a similar time frame, producing a nearly constant volume (inertially confined) reaction. Compression waves generated from this explosion transition to shocks and preheat an induction zone of fluid between the lead shock and the reacted fluid. In addition to the previous work [1, 2] spontaneous ignition of the induction zone has been observed by others both experimentally [3] and numerically [4]. The previous one-dimensional simulations focused on activation energies in the range 10 – 13.8, while more realistic activation energies can be as high as 100. Recent 1-D results [5] demonstrate that initiation still occurs with increased activation energy, but that a more incremental set of localized explosions occur similar to the theory proposed by [6]. This work examines the acoustic timescale mechanism in two dimensions and focuses on the differences in gasdynamic behavior between 1-D and 2-D simulations.

2 Problem Statement and Methodology

The non-dimensional 2-D reactive Euler equations are used to simulate detonation initiation. The equations are written in terms of the conserved quantities ρ , ρu_k , total energy ρe_T and fuel density ρY_F

$$\frac{\partial \rho}{\partial t} + \frac{\partial \rho u}{\partial x} = 0 \quad (1)$$

$$\frac{\partial \rho u}{\partial t} + \frac{\partial}{\partial x}(\rho u^2 + P) = 0 \quad (2)$$

$$\frac{\partial \rho e_T}{\partial t} + \frac{\partial}{\partial x}(\rho e_T + P)u = Q + Wq \quad (3)$$

$$\frac{\partial \rho Y}{\partial t} + \frac{\partial \rho Y u}{\partial x} = -W. \quad (4)$$

The equation of state and reaction rate are defined

$$\rho e_T = \frac{p}{\gamma - 1} + \frac{1}{2} \rho u^2 \quad (5)$$

$$W = B \rho Y \exp(-E/T). \quad (6)$$

The reaction rate W is modeled after a simple Arrhenius reaction rate where B is the pre-exponential factor, E is the activation temperature and $T = p/\rho$. Two additional source terms Q and (Wq) are added to the energy equation for the thermal power deposition and chemical energy release.

The variables use the same non-dimensionalization in [2] where the thermodynamic variables (p , ρ , T) are expressed with respect to the undisturbed dimensioned initial state (p'_o , ρ'_o , T'_o), where the subscript “ o ” indicates the initial state and prime indicates a dimensioned quantity. The entire non-dimensionalization is premised on a characteristic length l' in the undisturbed fluid such that the acoustic timescale $t'_A = l'/a'_o$, where $a'^2_o = \gamma R' T'_o$ and $\gamma = C'_p/C'_v$.

Each simulation begins with the reactive gas at rest in thermal equilibrium with initial condition

$$\rho_o = p_o = Y_o = 1 \quad u_{ko} = 0 \quad (7)$$

with transient thermal power deposition Q

$$Q = 4.2 \left(\tanh \left[5(t - t_a) \right] - \tanh \left[5(t - t_b) \right] \right) g(x_k) \quad (8)$$

The geometric term $g(x_k)$ limits the power addition to a circle of radius 2 centered at $x = 0$. The domain lies in $x \in [-3, 93]$ and $y \in [-3, 12]$ and reflecting slip walls are present on all walls except the exit $x = 93$. Each simulation uses a heat of reaction $q = 15$, specific heat ratio $\gamma = 1.4$ and activation temperature $E = 13.8$. Heat is added between $t_a = 0.5$ and $t_b = 5.25$.

Two separate simulations are presented where one has a pre-exponential factor $B = 35$ and successfully initiates a detonation while the second $B = 15$ does not form a detonation wave. Based on the previous work the steps leading to detonation formation include (1) thermal power deposition, (2) an initial explosion and generation of compression waves, (3) an induction period with shock interaction with the reacted fluid, (4) a localized explosion and (5) overdriven detonation wave formation. The events that occur beyond detonation formation are out of the scope of this work. Case 1 with $B = 35$ uses a grid spacing $\Delta x = \Delta y = 0.015$ on the finest level and Case 2 with $B = 15$ uses $\Delta x = \Delta y = 0.03$. The dynamically Adaptive Wavelet-Collocation Method (AWCM) is used in combination with a hyperbolic solver to perform the simulations [7].

3 Results

Case 1 begins with the power deposited in a cylinder and an explosion follows. This explosion produces a strong cylindrical compression wave that propagates away from the source as shown in the $t = 2$ pressure contour shown in Figure 1. It is hard to tell from the contour but at $t = 2$ the lead shock has already decoupled from the reacted medium.

The compression wave reflects off the three adiabatic walls producing a geometrically complex post-reflection shock wave. The reflected wave originating from the corner is incident upon the edge of the reacted deposition region and induces a Richtmyer-Meshkov instability, which deforms the reacted region. At $t = 5$ the lead shock front emerges from the reacted region and is about to reach the upper boundary. When reflection occurs on the upper boundary, substantial local inertial confinement occurs,

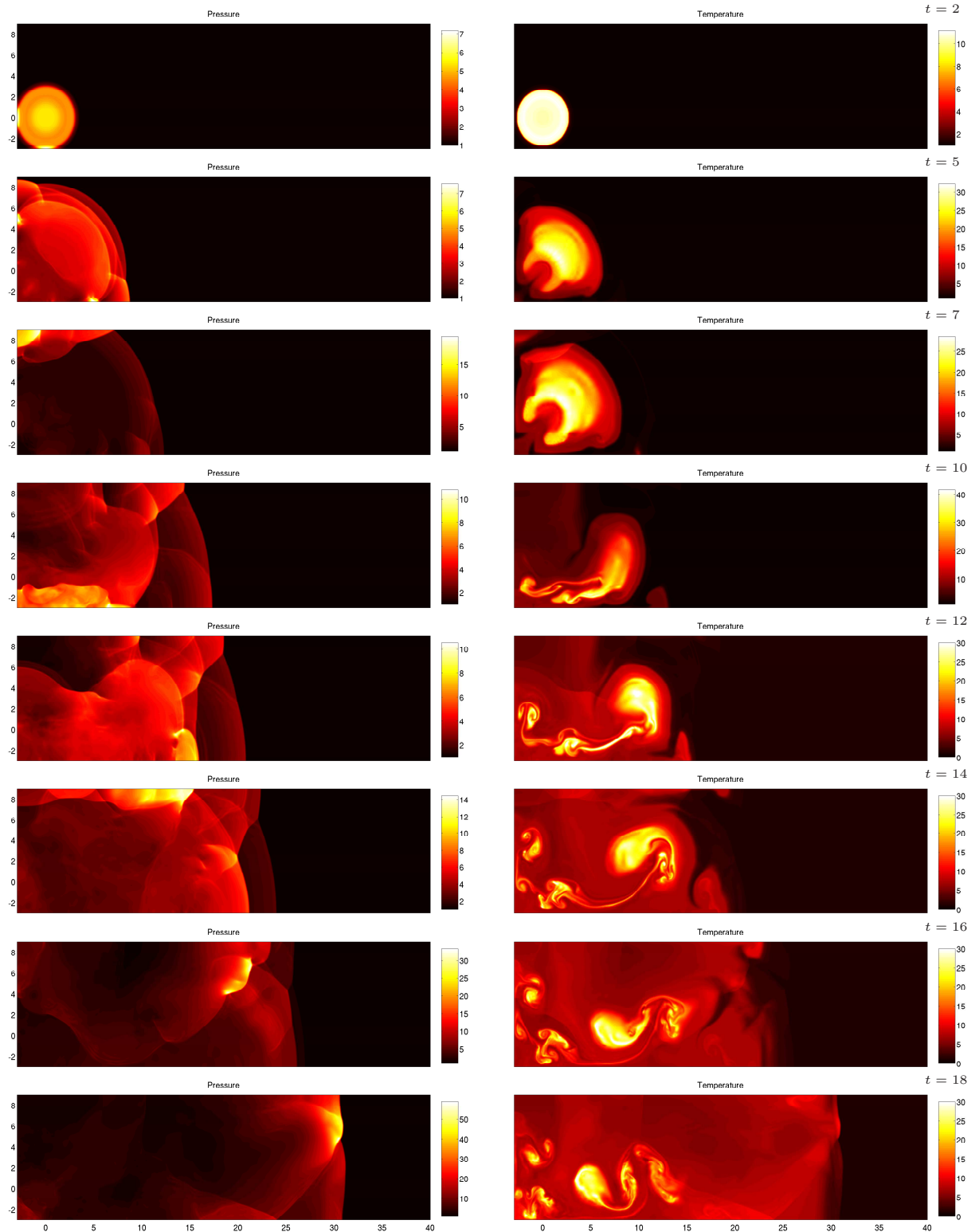


Figure 1: Pressure and temperature contour plots for output times $t = 2, 5, 7, 10, 12, 14, 16, 18$. The lead shock front decouples from the reaction zone and creates a large unreacted induction region between the reacted hot bubble and the lead shock. A spontaneous explosions occurs at $t = 14$ above the reacted bubble which accelerates until it reaches the lead shock as an overdriven detonation.

which produces a localized hot spot in the upper left corner of the channel. This hot spot explodes and locally amplifies the lead shock front. At $t = 7$, the reflected wave then re-enters the reacted region and is refracted, which induces an additional longitudinal component to the wave direction. Creation of additional longitudinal compression waves through transverse wave refraction inside the reacted fluid medium is a mechanism not present in the previous 1-D work [2, 5]. At $t = 10$ the unreacted multiply shocked region of warm fluid located $x \in [4, 15]$ has a temperature gradient in the $+x$ direction with an average temperature $T_l \approx 2$ so that the local acoustic timescale for this fluid region is $t_{AI} = l/\sqrt{T_l} = 11/\sqrt{2} = 7.8$.

Figure 1 shows when $t = 12$ and $t = 14$ this region of fluid spontaneously reacts in a time $t_{HI} = 4$ time units so that the ratio of heat release time to local acoustic time is $t_{HI}/t_{AI} = 0.51$. This suggests that moderate inertial confinement will occur, which is evidenced by the compression wave observed in the $t = 14$ temperature contour. The interaction of transverse waves with the walls induces a localized confinement that often results in temperature rises sufficient to form localized hot spots. This phenomena has been observed in both laboratory and numerical experiments [8–10]. Beyond $t = 14$ the entire preheated region behind the lead shock front reacts in another 4 time units and the accelerating wave propagates to the lead shock front where it emerges as an overdriven detonation wave.

For Case 2 the activation energy is the same as the previous case, but the pre-exponential factor is $B = 15$. A similar sequence of transient events occur for this case with the exception that the localized explosion located in the upper left corner of the previous case at $t = 7$ is absent in this case. With the lowered pre-exponential factor the peak pressure generated from original chemical explosion is only 5.5 whereas the previous case has a peak pressure of 7.5. This reduction in shock wave strength creates much longer fluid induction times and no localized explosion occurs.

At $t = 30$, Figure 2 shows in the upper left hand corner an isolated region of fluid from the primary distorted reacted bubble of fluid created by the initial explosion. This fluid reacted on a timescale greater than the local acoustic time and did not produce compression waves that could further increase the temperature of the reactants. Figure 2 shows that at $t = 40$ and $t = 60$ no localized explosion has occurred on timescales short enough to produce compression waves. Since the current work uses the Euler equations and is only concerned with gasdynamic behavior, hot spot formation inside of a flame brush described by [4] falls outside the scope of the current work. Although detonation initiation does not occur through gasdynamic heating in this case, it may still occur through other mechanisms if physical diffusion is present.

4 Conclusions

The 2-D simulations exhibit the same general gasdynamic behavior leading to detonation initiation observed in 1-D simulations. The primary difference between 1-D and 2-D is the role of transverse waves. Transverse waves reflect off of the top and bottom walls and are refracted as they enter the hot products region producing successive longitudinal compression waves that can further preheat the reactants. Similar to the 1-D simulations, an induction zone of warm fluid forms and inertial confinement occurs when a localized volume of fluid spontaneously releases its chemical energy on a timescale shorter than the local acoustic timescale, which creates a compression wave that accelerates through the temperature gradient until it reaches the lead shock front and produces an overdriven detonation wave.

In the case with reduced pre-exponential factor the initial explosion created by the thermal power deposition creates compression/shock waves with smaller post-shock temperatures and pressures. The reactants are heated to temperatures where the induction time is long compared to the time available in the numerical simulation. It is possible that in this case other DDT mechanisms may accelerate the process faster than a pure gasdynamic process.

References

- [1] A. A. Sileem, D. R. Kassoy, and A. K. Hayashi, “Thermally initiated detonation through deflagration to detonation transition,” *Proc. R. Soc. Lond. A*, vol. 435, pp. 459–482, 1991.
- [2] D. R. Kassoy, J. A. Kuehn, M. W. Nability, and J. F. Clarke, “Detonation initiation on the microsecond time scale: Ddts,” *Combustion Theory and Modeling*, vol. 12, no. 6, pp. 1009–1047, 2008.
- [3] A. Oppenheim and P. Urtiew, “Experimental observations of the transition to detonation in an explosive gas,” *Proc. Roy. Soc. A*, vol. 295, pp. 13–28, 1966.
- [4] A. M. Khokhlov and E. Oran, “Numerical simulation of detonation initiation in a flame brush: The role of hot spots,” *Combustion and Flame*, vol. 119, pp. 400–416, 1999.
- [5] J. D. Regele, D. R. Kassoy, and O. V. Vasilyev, “On the effect of increased activation energy in acoustic timescale detonation initiation,” *paper in progress*, 2011.
- [6] L. Bauwens and Z. Liang, “Shock formation ahead of hot spots,” in *Proceedings of the Combustion Institute*, vol. 29, 202, pp. 2795–2802.
- [7] J. D. Regele and O. V. Vasilyev, “An adaptive wavelet-collocation method for shock computations,” *International Journal of Computational Fluid Dynamics*, vol. 23, no. 7, pp. 503–518, 2009.
- [8] V. N. Gamezo, A. M. Khokhlov, and E. S. Oran, “The influence of shock bifurcations on shock-flame interactions and ddt,” *Combustion and Flame*, vol. 126, pp. 1810–1826, 2001.
- [9] A. M. Khokhlov and E. S. Oran, “Numerical simulation of detonation initiation in a flame brush: The role of hot spots,” *Combustion and Flame*, vol. 119, pp. 400–416, 1999.
- [10] A. K. Oppenheim, *Introduction to Gasdynamics of Explosions*. Springer-Verlag, New York, 1970.

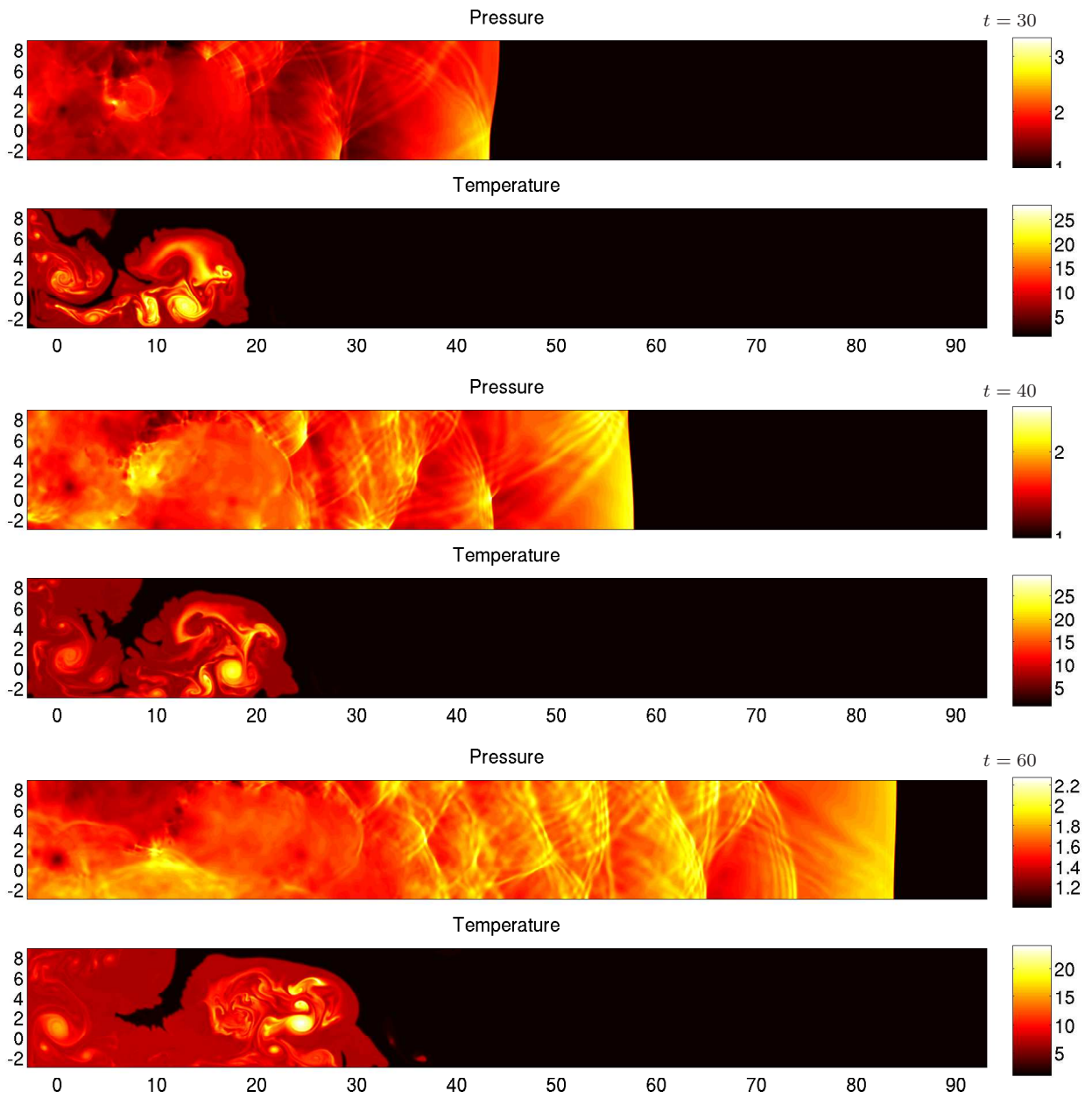


Figure 2: Pressure and temperature plots for output times $t = 30, 40$ and 60 show that detonation initiation does not occur for this case through gasdynamic processes.